

Synthesis and nuclear magnetic resonance investigation of 1-phenylpropane-1,2-dione 2-oxime complexes of trimethylplatinum(IV)

Peter J. Heard^{*a} and Kenneth Kite^b

^a Department of Chemistry, University of Wales, Swansea, Singleton Park, Swansea SA2 8PP, UK

^b Department of Chemistry, University of Exeter, Exeter EX4 4QD, UK

The ionised monoxime 1-phenylpropane-1,2-dione 2-oximate (ppdm) reacted smoothly with trimethylplatinum(IV) sulfate in aqueous acetone to form the complex *fac*-[PtMe₃(ppdm)(H₂O)] **1** in high yield. Complex **1** reacted with 3,5-dimethylpyridine (dmpy) and 2,2'-bipyridine (bipy) to form stable 1 : 1 adducts, *viz.* *fac*-[PtMe₃(ppdm)(dmpy)] **2** and *fac*-[PtMe₃(ppdm)(bipy)] **3**. In complexes **1** and **2** the ionised monoxime behaves as a N,O bidentate chelate, whereas in **3** ppdm is co-ordinated to the metal in a monodentate fashion, *via* the N-donor atom. The parent complex **1** dissolves in polar solvents to form species of general formulae *fac*-[PtMe₃(ppdm)(solv)] (solv = Me₂SO, methanol or acetone), which undergo an intramolecular 'windscreen-wiper' fluxional rearrangement. The stereodynamics of the fluxional process have been measured in CD₃OD and (CD₃)₂SO solution by two-dimensional exchange spectroscopy; ΔG^\ddagger (298 K) is 73.6 kJ mol⁻¹ and 88.5 kJ mol⁻¹, respectively. The effects of the solvent on the energetics and a possible mechanism for the fluxional process are discussed.

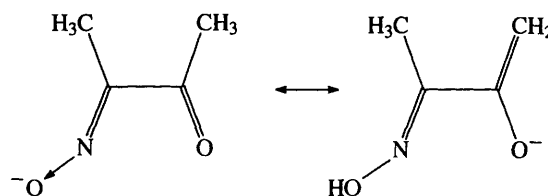
In a previous study¹ of trimethylplatinum(IV) complexes of the physiologically active monoxime butane-2,3-dione monoxime (Hbdm),² it was shown that, in the three complexes prepared, *viz.* [PtMe₃(bdm)]₂, [PtMe₃(bdm)(py)] (py = pyridine) and [PtMe₃(bdm)(bipy)] (bipy = 2,2'-bipyridine), the ionised ligand (bdm) adopted three different modes of co-ordination. Furthermore, in the parent complex, [PtMe₃(bdm)]₂, the oximate ligand appears to display two different configurations; an ionised hydroxy-oxime configuration in the solid state and in protic solvents, and a carbonyl-oxime configuration in aprotic solvents (Scheme 1).

The parent complex, [PtMe₃(bdm)]₂, is soluble only in co-ordinating solvents (solv), in which it dissociates into solvent-bonded monomeric species, [PtMe₃(bdm)(solv)]. The resulting complexes (solv = dimethyl sulfoxide, methanol or acetone) were shown to undergo a novel 'windscreen-wiper' fluxional rearrangement. The energetics of the rearrangement were measured by two-dimensional exchange spectroscopy (EXSY) in [D₂H₄]methanol; ΔG^\ddagger (298 K) was *ca.* 74 kJ mol⁻¹. It was therefore of interest to study the behaviour of the related monoxime, 1-phenylpropane-1,2-dione 2-oxime (Hppdm), which can only adopt a carbonyl-oxime configuration when ionised. As with Hbdm, few complexes of Hppdm have been reported hitherto. Aromatic carbonyl oximes are generally regarded as poor chelating agents, and the complexes, if formed at all, are usually unstable.^{3,4} The crystal structure of the cobalt(III) complex, [Co(ppdm)]₃, has been reported,⁴ and is presumably the same compound as that described as the characterisation product of the ligand.⁵ In contrast, like Hbdm, ionised 1-phenylpropane-1,2-dione 2-oximate (ppdm) reacts readily with trimethylplatinum(IV) sulfate in aqueous media to form a stable Pt-N=C-C=O chelated complex. The parent complex, [PtMe₃(ppdm)] **1**, which is monomeric (with a water molecule occupying the sixth co-ordination site), reacts readily with 3,5-dimethylpyridine and 2,2'-bipyridine in benzene, to form the 1 : 1 adducts, [PtMe₃(ppdm)(dmpy)] **2** and [PtMe₃(ppdm)(bipy)] **3**, respectively.

Experimental

Materials

1-Phenylpropane-1,2-dione 2-oxime was obtained from Aldrich



Scheme 1 The two possible configurations for ionised butane-2,3-dione monoxime

Chemical Company and used without further purification. Trimethylplatinum(IV) sulfate was prepared by our previously published procedure.¹

Syntheses

[PtMe₃(ppdm)(H₂O)] **1**. 1-Phenylpropane-1,2-dione 2-oxime (800 mg, 0.49 mmol) was added as a solid to a stirred aqueous acetone solution (50 : 50 v/v) of trimethylplatinum(IV) sulfate, [(PtMe₃)₂SO₄·4H₂O] (500 mg, 0.77 mmol). Sodium acetate trihydrate (0.50 g, 3.67 mmol) was added to the resulting clear orange solution. The reaction mixture was stirred for *ca.* 0.5 h, during which time an orange solid precipitated. The solid was filtered off, washed with water and dried *in vacuo*. Recrystallisation from acetone-hexane gave 390 mg (60%) of pure orange [PtMe₃(ppdm)(H₂O)].

[PtMe₃(ppdm)(dmpy)] **2**. 3,5-Dimethylpyridine (0.20 cm³) was added to a stirred suspension of [PtMe₃(ppdm)(H₂O)] (100 mg, 0.24 mmol) in benzene (10 cm³). The reaction mixture was stirred for *ca.* 1.5 h. The resulting pale pink solution was then evaporated to dryness *in vacuo* and the solid residue crystallised from benzene-hexane to yield a red-pink solid. Yield 78 mg, 64%.

[PtMe₃(ppdm)(bipy)] **3**. 2,2'-Bipyridine (0.150 mg, 0.64 mmol) was added to a stirred suspension of [PtMe₃(ppdm)(H₂O)] (150 mg, 0.37 mmol) in benzene (15 cm³). After *ca.* 3 h of stirring at ambient temperature a clear yellow solution was obtained. Concentration of the mother-liquor to *ca.* 5 cm³ *in vacuo* and addition of hexane yielded crystalline, yellow [PtMe₃(ppdm)(bipy)]. Yield 162 mg, 81%.

Physical methods

Hydrogen-1 NMR spectra were recorded in [$^2\text{H}_6$]dimethyl sulfoxide, [$^2\text{H}_4$]methanol, [$^2\text{H}_6$]acetone or CDCl_3 solution, on either a Bruker AC300 or a Bruker AC400 Fourier-transform spectrometer, operating at 300.13 and 400.13 MHz, respectively. Chemical shifts are quoted in ppm, relative to tetramethylsilane as an internal standard. The probe temperatures were controlled by a standard B-VT 2000 unit; temperatures were checked periodically against a standard sample of methanol in [$^2\text{H}_4$]methanol, and are considered accurate to within $\pm 1^\circ\text{C}$. Two-dimensional exchange spectra were obtained using the Bruker NOESYPH program,⁶ which generates the pulse sequence $\text{D1}-90^\circ-\text{D0}-90^\circ-\text{D9}-90^\circ$ -free induction decay. Spectra were typically recorded with 512 words of data in f_1 and f_2 , and transformed with 1024 words of data. The initial delay, D0, was set at 3 μs and the relaxation delay, D1, was 2.0 s. The mixing time, D9, was varied according to the complex under investigation, and the experimental temperature. Signal intensities were obtained from the resulting two-dimensional spectra by volume integration. Integrations were performed five times; mean values were used to determine the exchange rates from the program D2DNMR.⁷ The activation parameters were calculated from a least-squares fit of the linearised Eyring and Arrhenius equations. Errors quoted are those defined by Binsch and Kessler.⁸

Infrared spectra were recorded as pressed CsI discs on a Nicolet Magna 550 FT-IR spectrometer, operating in the region $4000-200\text{ cm}^{-1}$. Fast atom bombardment (FAB) mass spectra were obtained on a VG AutoSpec instrument using caesium-ion bombardment at 25 kV energy, on samples of the complexes dissolved in a matrix of 3-nitrobenzyl alcohol. Elemental analyses were carried out at Butterworth Laboratories Ltd., Teddington, Middlesex.

Results and Discussion

The three complexes $[\text{PtMe}_3(\text{ppdm})(\text{H}_2\text{O})]$ **1**, $[\text{PtMe}_3(\text{ppdm})(\text{dmpy})]$ **2** and $[\text{PtMe}_3(\text{ppdm})(\text{bipy})]$ **3**, were prepared in high yields as described (see above). The analytical data (see below) indicate that the complexes have the structures shown. Attempts to prepare the dimer, $[\{\text{PtMe}_3(\text{ppdm})\}_2]$, by dehydration of **1** were unsuccessful, as were those to prepare the pyridine adduct, $[\text{PtMe}_3(\text{ppdm})(\text{py})]$.

The infrared spectrum of complex **1**, showed a strong, broad band at 3243 cm^{-1} (the half-height line width $\Delta\sigma_{\frac{1}{2}} = 220\text{ cm}^{-1}$), which shifted to 2360 cm^{-1} ($\Delta\sigma_{\frac{1}{2}} = 880\text{ cm}^{-1}$) on deuteration of the complex. Since no NOH configuration is possible for the ionised monoxime ligand, this indicates the presence of a co-ordinated water molecule. Three bands were observed in the C-H stretching region,⁹⁻¹² two due to C-H stretching modes and one due to the overtone of the C-H deformation at *ca.* 1408 cm^{-1} . One Pt-N and three Pt-C stretching modes were also tentatively assigned. The strong band at 1552 cm^{-1} was assigned to the C=O stretch of the co-ordinated oximate carbonyl group. These data are consistent with **1** having the structure shown. Infrared data are reported in Table 1.

The infrared spectrum of the 3,5-dimethylpyridine adduct, **2**, displayed three bands in the C-H stretching region, together with one Pt-N and three Pt-C stretching bands. The signal at 1520 cm^{-1} was assigned to the oximate carbonyl stretching mode. Complex **3** displayed three bands in the C-H stretching region, three Pt-C and two Pt-N stretching bands. The presence of a band at 1622 cm^{-1} , assigned to the stretching mode of a free carbonyl group, indicates that the monoximate oxygen donor atom is unco-ordinated. The infrared data for **2** and **3** (Table 1) thus indicate that the complexes have the structures depicted.

Fast atom bombardment mass spectrometry was performed on the three complexes, **1-3**. The parent complex, **1**, displayed

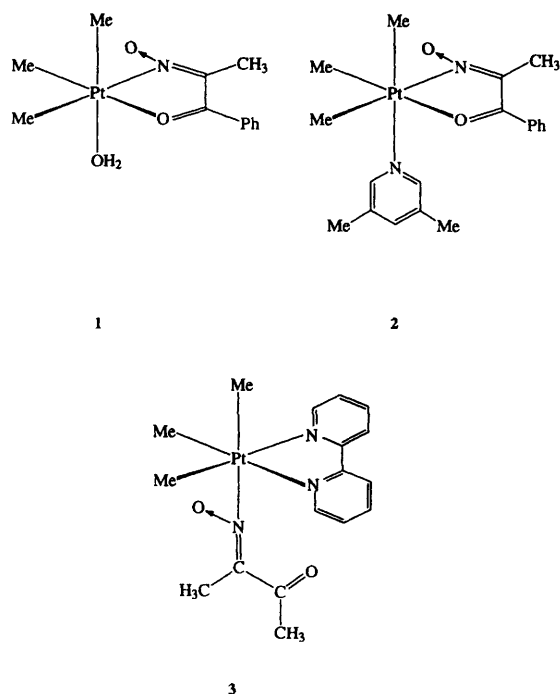


Table 1 Analytical data for complexes **1-3**

Complex	IR ^a /cm ⁻¹			Analysis ^c (%)		
	$\nu(\text{C-H})$	$\nu(\text{Pt-C})$	$\nu(\text{Pt-N})^b$	C	H	N
1	2817	561	437	34.45	3.85	3.30
	2899	580		(34.3)	(4.55)	(3.35)
	2961	596				
2	2816	568	445	44.95	4.95	5.35
	2894	584		(44.8)	(5.15)	(5.50)
	2952	600				
3	2815	573	422	48.55	3.95	7.60
	2894	585	434 (sh)	(47.3)	(4.50)	(7.55)
	2956	595				

^a Recorded as pressed CsI discs; sh = shoulder. ^b Not all bands observed. ^c Calculated figures in parentheses.

an intense peak at m/z 403, which corresponds to the species $[\text{M} - \text{OH}]^+$; this presumably arises from protonation of $[\text{PtMe}_3(\text{ppdm})]$, *i.e.* $\text{M} - \text{OH}_2$. Strong fragmentation peaks were also observed at m/z 357 $[\text{Pt}(\text{ppdm})]$ and 240 (PtMe_3) . The 3,5-dimethylpyridine adduct, **2**, displayed a molecular ion at m/z 509 (*M*), with further strong peaks at m/z , 464 $[\text{Pt}(\text{ppdm})(\text{dmpy})]$, 347 $[\text{PtMe}_3(\text{dmpy})]$, 317 $[\text{PtMe}(\text{dmpy})]$ and 302 $[\text{Pt}(\text{dmpy})]$. Complex **3**, $[\text{PtMe}_3(\text{ppdm})(\text{bipy})]$, displayed intense signals at m/z 581, 559, 396, 366 and 350, attributable to the species $[\text{M} + \text{Na}]$, $[\text{M}]$, $[\text{PtMe}_3(\text{bipy})]$, $[\text{PtMe}_2(\text{bipy})]$ and $[\text{PtMe}(\text{bipy})]$ respectively. In *all* cases the observed isotope distribution patterns were in accord with those calculated for the formulated species.

The elemental analyses (Table 1) obtained for complexes **1-3** were generally consistent with the formation of analytically pure complexes; however, the somewhat anomalous C and H analyses for the 2,2'-bipyridyl adduct **3** were difficult to rationalise.

NMR Studies on $[\text{PtMe}_3(\text{ppdm})(\text{H}_2\text{O})]$ **1**

Complex **1** dissolves in polar solvents, forming a solvent co-ordinated species, *viz.* $[\text{PtMe}_3(\text{ppdm})(\text{solv})]$. In $(\text{CD}_3)_2\text{SO}$ solution the ambient-temperature (298 K) ^1H NMR spectrum (Fig. 1) shows well resolved signals. The platinum-methyl

Table 2 Hydrogen-1 NMR data^a for complexes **1** and **1b**

Complex	Solvent	T/K	$\delta(\text{Pt}-\text{CH}_3)^b$	<i>trans</i> Atom	$\delta(\text{Pt}-\text{O}=\text{C}-\text{C}_6\text{H}_5)^{c,d}$
1 ^e	$(\text{CD}_3)_2\text{SO}$	298	0.68(69.2)	S (Me_2SO)	7.56(≈ 7.0) H_m
			0.86(64.0)	N (oximate)	7.63(≈ 7.0 ; 1.4) H_p
			1.20(76.4)	O (oximate)	7.74(≈ 7.0 ; 1.4) H_o
	CD_3OD	270	0.70(83.1)	O (methanol)	7.57(≈ 7.0) H_m
			0.94(63.3)	N (oximate)	7.64(≈ 7.0 ; 1.5) H_p
			1.17(76.5)	O (oximate)	7.77(≈ 7.0 ; 1.5) H_o
	$(\text{CD}_3)_2\text{CO}$	243	0.60(83.9) ^f	O (H_2O)	
			0.87(63.1) ^f	N (oximate)	
			1.13(76.3) ^f	O (oximate)	
0.76(84.6) ^g			O (acetone)		
0.88(62.3) ^g			N (oximate)		
1.19(75.4) ^g			O (oximate)		
1b	$(\text{CD}_3)_2\text{CO}$	238	0.53(82.8)	O (D_2O)	
			0.85(63.6)	N (oximate)	
				O (oximate)	
			1.11(76.8)	O (oximate)	

^a Chemical shifts quoted relative to SiMe_4 as an internal standard. ^b $^2J_{\text{PtH}}$ /Hz given in parentheses. ^c Data for complex **1** in acetone could not be measured precisely due to overlapping signals (see text); data for **1b** not measured. ^d $^3J_{\text{HH}}$ /Hz; ^e $^4J_{\text{HH}}$ /Hz given in parentheses. ^e In $(\text{CD}_3)_2\text{SO}$, $\delta(\text{Pt}-\text{N}=\text{C}-\text{CH}_3)$ 1.89 ($^4J_{\text{PtH}} \approx 4$); in CD_3OD , 2.05 (3.8 Hz). ^f Data for the major isomer, $[\text{PtMe}_3(\text{ppdm})(\text{H}_2\text{O})]$ (54%) (see text). ^g Data for the minor isomer, $[\text{PtMe}_3(\text{ppdm})\{(\text{CD}_3)_2\text{CO}\}]$ (46%) (see text).

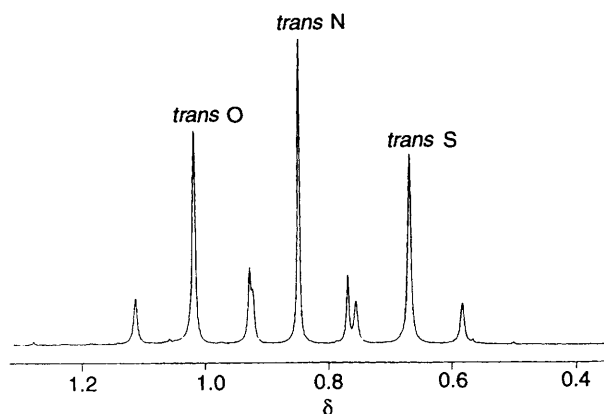
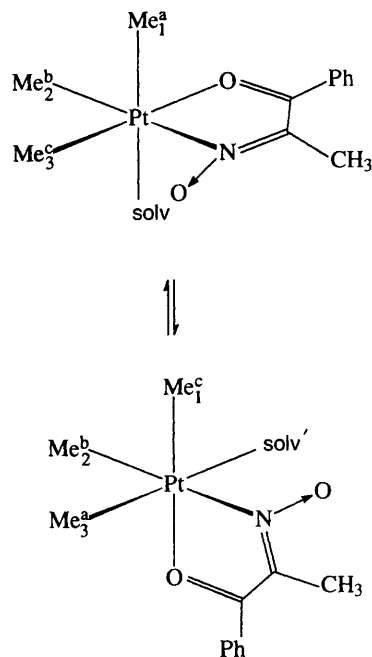


Fig. 1 The 400 MHz ^1H NMR spectrum of complex **1** in $(\text{CD}_3)_2\text{SO}$ at 298 K, showing the platinum-methyl region. See Table 2 for assignments

region (*ca.* δ 0.5–1.2) displayed three signals, with ^{195}Pt satellites, in a 1 : 1 : 1 intensity ratio. On the basis of their $^2J_{\text{PtH}}$ scalar coupling constants,^{1,13–16} these signals were assigned to methyls *trans* to O (oximate), N (oximate) and S (Me_2SO), respectively from high to low frequency. The low magnitude for the $^2J_{\text{PtH}}$ scalar coupling constant for the *trans* N (oximate) methyl group {64.0 Hz, *cf.* 66.5 Hz for $[\text{PtMe}_3(\text{bipy})(\text{H}_2\text{O})]^{9}$ } indicates the presence of a strong Pt–N interaction. The ligand-methyl region ($\text{Pt}-\text{N}=\text{C}-\text{CH}_3$) showed a single resonance, with ^{195}Pt coupling. The signals due to the ligand-phenyl ring ($\text{Pt}-\text{O}=\text{CPh}$) could also be fully assigned (Table 2).

On warming the solution a number of reversible band-shape changes occurred, indicating the onset of dynamic exchange processes at a measurable rate on the NMR chemical shift time-scale. First, the signal due to the PtMe group *trans* to (Me_2SO) broadened and shifted slightly to higher frequency; this was accompanied by a small increase in the $^2J_{\text{PtH}}$ coupling, indicating a lengthening and weakening of the platinum-solvent interaction. This signal then sharpens again, as the complex attains a rapid pre-equilibrium (which probably involves solvent exchange). On warming further, the signals *trans* to O (oximate) and to S (Me_2SO) displayed dynamic line broadening, due to the expected¹ windscreen-wiper fluxional rearrangement (Scheme 2). Line-shape changes characteristic of platinum-methyl scrambling, a well established feature of fluxional trimethylplatinum(IV) complexes,¹² also occurred at elevated temperatures. No changes were observed in the other regions of the spectra; the $^4J(\text{Pt}-\text{N}=\text{C}-\text{CH}_3)$ scalar coupling (*ca.*



Scheme 2 The ‘windscreen-wiper’ fluxional rearrangement of complex **1**, showing the effects of the fluxional process on the platinum methyls. The numbers refer to the three sites of the *fac*-oriented methyl groups, and the letters identify the chemical environments

4 Hz) was unaffected by the dynamic processes, indicating that the Pt–N bond remains intact at all times.

The energetics of the windscreen-wiper fluxion were measured by two-dimensional exchange spectroscopy. Five EXSY experiments were performed* at temperatures at which the pre-equilibrium had been attained, but the PtMe scrambling was of negligible rate on the NMR magnetisation-transfer time-scale. Reliable rate data were obtained (Table 3), and the activation parameters for the windscreen-wiper rearrangement determined (Table 4). The two-dimensional EXSY spectrum of complex **1** in $(\text{CD}_3)_2\text{SO}$ at 323 K is shown in Fig. 2.

The ambient-temperature (298 K) spectrum of complex **1** in $[\text{H}_4]\text{methanol}$ revealed slightly exchange-broadened signals; this broadening disappeared on cooling to *ca.* 273 K and a well resolved spectrum was obtained. The ‘static’ spectrum was

* On 14 mg of complex **1** dissolved in 0.5 cm^3 of the deuteriated solvent; the same sample was used for each of the five experiments.

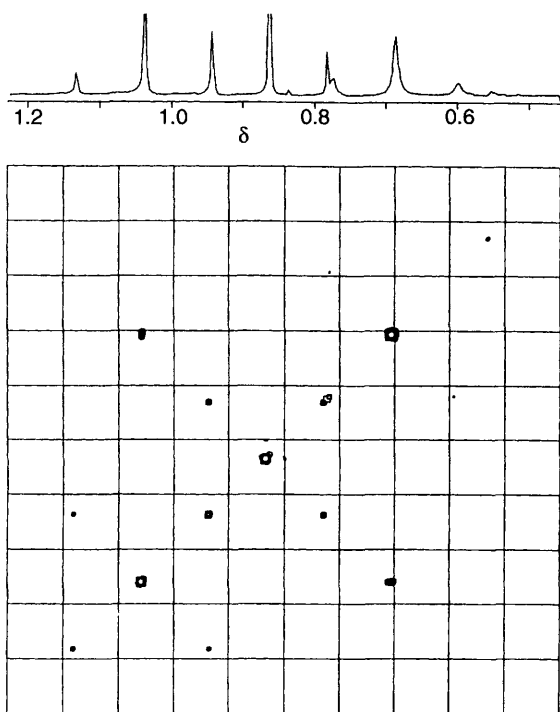


Fig. 2 The 400 MHz two-dimensional exchange ^1H NMR spectrum of complex **1** in $(\text{CD}_3)_2\text{SO}$ at 323 K. Cross-peaks are displayed between the platinum methyls *trans* to solvent and to O (oximate). Further weak cross-peaks occur between the platinum satellites of each of the signals

exactly analogous to that of **1** in $(\text{CD}_3)_2\text{SO}$. Hydrogen-1 NMR data are reported in Table 2. On warming, changes in the PtMe band shapes consistent with (i) the attainment of a pre-equilibrium, followed by (ii) the expected windscreen-wiper fluxion and (iii) PtMe scrambling (see above) were observed. The energetics of the windscreen-wiper fluxional rearrangement were measured by two-dimensional exchange spectroscopy; five EXSY experiments were performed in the temperature range 297–313 K, and reliable rate data obtained (Table 3). The Eyring and Arrhenius activation parameters are reported in Table 4.

In $[\text{H}_6]\text{acetone}$ the ambient-temperature (298 K) spectrum of complex **1** showed extensive line broadening. On cooling to 243 K the band shapes sharpened to reveal a total of six platinum–methyl signals (with ^{195}Pt satellites), resulting from two solution-state species; each species displayed three signals in a 1:1:1 intensity ratio. The relative populations of the two species are highly temperature dependent. The two sets of signals are believed to arise from the presence of both an acetone-co-ordinated complex and a water-co-ordinated complex. The presence of the latter in acetone solution was not totally unexpected, because **1** is crystallised as the H_2O adduct from acetone (see above).

The addition of an excess of D_2O to the $[\text{H}_6]\text{acetone}$ solution of complex **1** at 238 K resulted in a single set of PtMe signals, which presumably arise from the D_2O adduct, $[\text{PtMe}_3(\text{ppdm})(\text{D}_2\text{O})]$ **1b**. The chemical shift and scalar coupling data for $[\text{PtMe}_3(\text{ppdm})(\text{D}_2\text{O})]$ (Table 2) were more closely analogous to the data for the major isomer at that temperature. This suggests that the major solution-state species is the H_2O adduct, $[\text{PtMe}_3(\text{ppdm})(\text{H}_2\text{O})]$; the spectrum of **1** was assigned on this basis. The ligand-methyl and -phenyl regions of the spectra each displayed two sets of overlapping signals due to the two species, *viz.* $[\text{PtMe}_3(\text{ppdm})(\text{H}_2\text{O})]$ and $[\text{PtMe}_3(\text{ppdm})\{(\text{CD}_3)_2\text{CO}\}]$; as a result, the chemical shifts and scalar coupling constants could not be measured with confidence. Hydrogen-1 NMR data are reported in Table 2. The spectrum of **1** in $[\text{H}_6]\text{acetone}$ at 243 K is shown in Fig. 3.

On warming the $[\text{H}_6]\text{acetone}$ solution of complex **1** the two

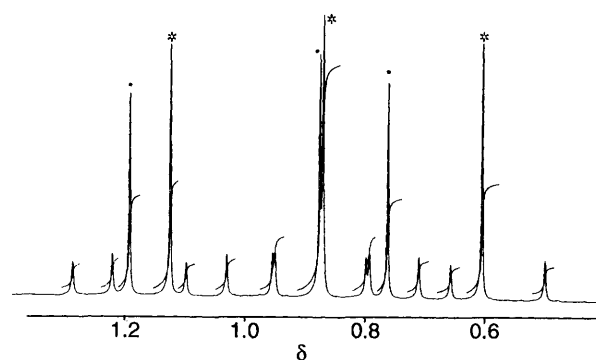


Fig. 3 The 400 MHz ^1H NMR spectrum of complex **1** in $[\text{H}_6]\text{acetone}$ at 243 K, showing the platinum–methyl region. The signals due to the major and minor isomers are labelled (*) and (-), respectively. See Table 2 for the assignments

Table 3 Two-dimensional EXSY data* for complex **1**

Solvent	<i>T</i> /K	Mixing time, D_9/s	k/s^{-1}
$(\text{CD}_3)_2\text{SO}$	323	1.50	0.08
	328	1.20	0.22
	334	1.00	0.58
	340	0.80	1.29
	345	0.20	1.56
CD_3OD	291	1.60	0.32
	297	1.00	0.65
	303	0.70	1.45
	308	0.20	2.46
	313	0.12	5.10

* First-order rate constants for the windscreen-wiper rearrangement. Uncertainties are *ca.* $\pm 5\%$.

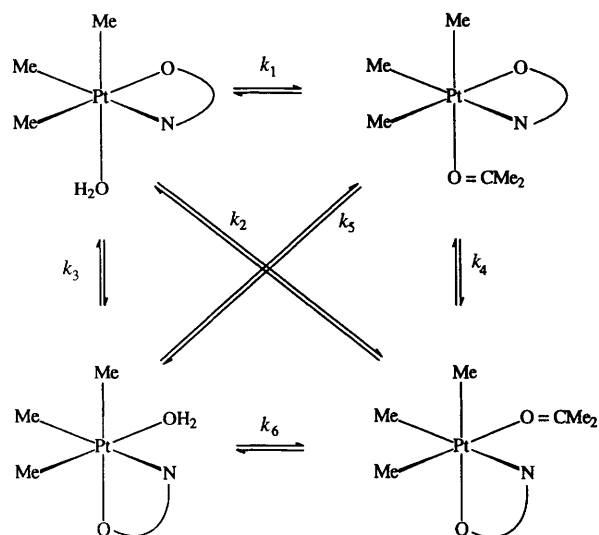
Table 4 Activation parameters* for complex **1**

Parameter	Solvent	
	$(\text{CD}_3)_2\text{SO}$	CD_3OD
$E_a/\text{kJ mol}^{-1}$	126.8(11.6)	94.1(2.9)
$\log_{10}(A/\text{s}^{-1})$	19.5(2.0)	16.4(0.5)
$\Delta H^\ddagger/\text{kJ mol}^{-1}$	124.0(11.6)	91.5(2.9)
$\Delta S^\ddagger/\text{J K}^{-1} \text{mol}^{-1}$	119.3(38.7)	60.1(9.7)
$\Delta G^\ddagger/\text{kJ mol}^{-1}$	88.5(1.4)	73.6(0.1)

* Errors given in parentheses; ΔG^\ddagger quoted at 298 K.

sets of PtMe signals broadened. The ^1H NMR band-shape changes indicated the onset of both an intermolecular exchange between the two solution-state species, and the expected windscreen-wiper rearrangement (in both species). Attempts to obtain accurate rate data were frustrated. The presence of four independent rate constants (see below), plus PtMe scrambling at elevated temperatures, renders simulation of standard one-dimensional NMR spectra unreliable; the band-shape changes cannot be fitted to a unique set of rate constants in such circumstances. Also the large difference in the magnitudes of the rate constants prevented their accurate measurement by two-dimensional EXSY; there was no mixing time which enabled the four independent rate processes (Scheme 3) to be measured simultaneously at a given temperature. However, from the two-dimensional EXSY experiments, it was found that the magnitudes for the four rate processes are in the order $k_1 > k_3 \approx k_4 > k_2$ (see Scheme 3).

The magnitude for the free energy of activation for the windscreen-wiper fluxional rearrangement of complex **1** in $[\text{H}_4]\text{methanol}$ (Table 4) is, within experimental error, the same as that obtained for the complex $[\text{PtMe}_3(\text{bdm})]$ in the same solvent.¹ Thus changing the nature of the monoxime has a negligible effect on the energy barrier of the process. In



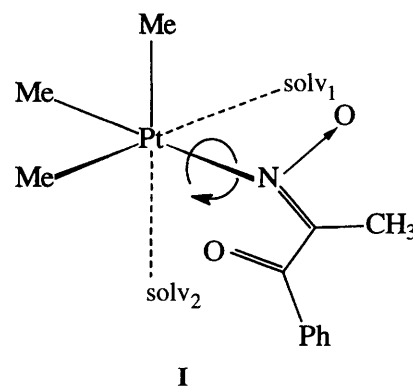
Scheme 3 The four solution-state species of the complex $[\text{PtMe}_3(\text{ppdm})(\text{H}_2\text{O})]$ in $[\text{}^2\text{H}_6]\text{acetone}$, and the six interconversion pathways between them. Note that $k_2 \equiv k_5$ and $k_1 \equiv k_6$, giving four independent rate processes

contrast, the effect of the different solvents is very marked. The rates of the windscreen-wiper fluxion for the complex species $[\text{PtMe}_3(\text{bdm})(\text{sol})]$ were shown qualitatively to be in the order¹ $\text{Me}_2\text{SO} < \text{MeOH} < \text{Me}_2\text{CO}$. Comparison of the magnitudes for ΔG^\ddagger (298 K) obtained for **1** in $(\text{CD}_3)_2\text{SO}$ and CD_3OD (Table 4) enables a quantitative estimate of the effect of the solvent on the windscreen-wiper rearrangement. The trend in the free energy of activation, *viz.* $\text{Me}_2\text{SO} > \text{Me}_2\text{CO}$, is in accord with the trend expected from the relative strengths of the Pt–E (solvent) interactions (E = S or O). A qualitative comparison of the relative strengths of these interactions can be made by inspection of the $^2J_{\text{PtH}}$ scalar couplings^{17,18} for the PtMe signals *trans* to solvent; the larger the scalar coupling constant, the weaker is the *trans* platinum–solvent interaction. The magnitudes for the $^2J_{\text{PtH}}$ scalar couplings are (Table 2) 69.2 [*trans* to S (Me_2SO)] and 83.1 Hz [*trans* to O (methanol)]; this lends support to the hypothesis that the mechanism of the rearrangement (see below) involves cleavage of the platinum–solvent bond. While it was not possible to obtain a value for the free energy of activation for the windscreen-wiper fluxion in $(\text{CD}_3)_2\text{CO}$ (see above), the (much) broader ^1H NMR band shapes observed at ambient temperature (298 K) clearly indicate that the rate of the rearrangement is more rapid in this solvent. The $^2J_{\text{PtH}}$ scalar coupling constant for the platinum–methyl group *trans* to acetone is also, as expected, greater (84.5 Hz at 233 K) than that for methyl group *trans* to solvent in either Me_2SO or methanol solution, indicating that the Pt–O (acetone) interaction is weaker.

Although caution should be exercised when interpreting entropy of activation data, the sizeable positive magnitudes of ΔS^\ddagger measured for the windscreen-wiper fluxion point to a transition state which is at least partially dissociated. However, even at fast rates of exchange, the $^4J(\text{Pt}=\text{N}=\text{C}-\text{CH}_3)$ scalar coupling is retained. The Pt–N (oximate) bond must therefore remain intact during the course of the rearrangement; this provides an insight into the mechanism of the fluxional process. Although the precise nature of the mechanism is not known, it is believed to involve cleavage of the Pt–O (oximate) bond, followed by a 45° rotation of the ligand about the Pt–N (oximate) bond and displacement of the solvent molecule (see above). A possible transition-state structure for the rearrangement is depicted in **I**.

NMR spectra of complexes **2** and **3**

The hydrogen-1 NMR spectrum of $[\text{PtMe}_3(\text{ppdm})(\text{dmpy})]$ **2**,



in CDCl_3 at 303 K showed three PtMe signals, with ^{195}Pt satellites, in a 1:1:1 intensity ratio. The assignment of these signals (Table 5) was based on the magnitudes of their $^2J_{\text{PtH}}$ scalar coupling constants.^{1,13–16} The signals at δ 1.92 (3 H) and 2.30 (6 H) were assigned to the oximate-methyl group ($^4J_{\text{PtH}} \approx 3.8$ Hz) and the two methyls of dmpy, respectively. The overlapping signals due to the oximate-phenyl ring hydrogen nuclides and the *p*-hydrogen of the dmpy ring were not fully resolved; this frustrated the measurement of reliable chemical shift and coupling-constant data. The signal at δ 8.16 was unambiguously assigned to the *o*-hydrogen nuclides of the dmpy ring, on account of their measurable coupling to platinum-195, $^3J_{\text{PtH}} \approx 11.1$ Hz.

The ^1H NMR spectrum of complex **3** in CDCl_3 at 303 K displayed two PtMe signals (with ^{195}Pt satellites) in a 2:1 intensity ratio; the $^2J_{\text{PtH}}$ scalar couplings (69.1 and 70.9 Hz, respectively) indicate that all three methyl groups are *trans* to N^{1,13–16} (*cf.* *trans* to O scalar couplings of *ca.* 80 Hz; see Table 2). The bipyridyl ligand must therefore be co-ordinated to the metal moiety in a bidentate chelate fashion, with the oximate bound only through the N-donor atom. The signal at δ 1.77 was assigned to the oximate-methyl group, on the basis of its chemical shift (see above); however, no ^{195}Pt satellites were observed, indicating that the magnitude of the long-range (4J) Pt–H coupling is strongly dependent on the conformation of the oximate ligand. This is in accord with data previously reported for the complex $[\text{PtMe}_3(\text{bdm})(\text{bipy})]$.¹ The α -hydrogens of the bipyridyl ring gave rise to a doublet, with ^{195}Pt satellites, at δ 8.65; $^3J_{\text{PtH}} \approx 11.9$ Hz. Overlap of the other aromatic signals prevented their unambiguous assignment. Hydrogen-1 NMR data for **3** are reported in Table 5.

Conclusion

Analytical and NMR data for the complexes $[\text{PtMe}_3(\text{ppdm})(\text{H}_2\text{O})]$ **1**, $[\text{PtMe}_3(\text{ppdm})(\text{dmpy})]$ **2** and $[\text{PtMe}_3(\text{ppdm})(\text{bipy})]$ **3**, are consistent with the complexes having the structures shown. The parent complex, **1**, dissolves in polar solvents to form a solvent-co-ordinated species, which undergoes a ‘windscreen-wiper’ fluxional rearrangement. The kinetics of the fluxional process are dominated by the strength of the Pt–E (solvent) (E = S or O) interaction, and appears to be essentially independent of the nature of monoximate ligand. We are currently investigating the behaviour of related N,O and N,S chelate ligand complexes of trimethylplatinum(IV) in order to establish whether or not the windscreen-wiper fluxional rearrangement occurs more generally.

Acknowledgements

We are grateful to the University of Wales at Swansea and the University of Exeter for financial support. Dr. V. Šik and Mr. W. M. Nettle are acknowledged for the acquisition of a number of the NMR spectra.

Table 5 Hydrogen-1 NMR data^a for complexes **2** and **3**

Complex	$\delta(\text{Pt}-\text{CH}_3)^b$	Integral	<i>trans</i> Atom	$\delta(\text{Pt}=\text{N}=\text{C}-\text{CH}_3)^c$	$\delta(\text{CH}_3 \text{ of dmpy})$	$\delta(\text{azine H})^d$
2	0.68(71.8)	3 H	N (dmpy)	1.92(3.8)	2.3	8.16(11.1)
	0.95(64.1)	3 H	N (oximate)			
	1.22(76.6)	3 H	O (oximate)			
3	0.21(70.9)	3 H	N (oximate)	1.77	—	8.65(11.9; 5.9)
	1.26(69.1)	6 H	N (bipy)			

^a Data recorded at 303 K in CDCl₃ solution. Chemical shifts quoted relative to SiMe₄ as an internal standard. ^b ²J_{PtH}/Hz in parentheses. ^c ⁴J_{PtH}/Hz in parentheses. ^d Data for the α -hydrogen nuclides; ³J_{PtH}/Hz; ³J_{HH}/Hz given in parentheses. Other aromatic signals not assigned (see text).

References

- 1 E. W. Abel, P. J. Heard, K. Kite, K. G. Orrell and A. F. Psaila, *J. Chem. Soc., Dalton Trans.*, 1995, 1233.
- 2 L. C. Sellin and J. J. McArdle, *Pharm. Toxicol.*, 1994, **74**, 305 and refs. therein.
- 3 A. Chakravorty, *Coord. Chem. Rev.*, 1974, **13**, 1.
- 4 H. Saarinen, J. Korvenranta and E. Näsäkkälä, *Acta Chem. Scand., Ser. A*, 1978, **32**, 33.
- 5 D. H. Hey, *J. Chem. Soc.*, 1930, 18.
- 6 G. Bodenhausen, H. Kogler and R. R. Ernst, *J. Magn. Reson.*, 1984, **58**, 34.
- 7 E. W. Abel, T. P. J. Coston, K. G. Orrell, V. Šik and D. Stephenson, *J. Magn. Reson.*, 1986, **70**, 34.
- 8 G. Binsch and H. Kessler, *Angew. Chem., Int. Ed. Engl.*, 1980, **19**, 411.
- 9 D. E. Clegg, J. R. Hall and G. A. Swile, *J. Organomet. Chem.*, 1972, **38**, 403.
- 10 J. R. Hall, *Essays in Structural Chemistry*, eds. A. J. Downs, D. A. Long and L. A. K. Staveley, Macmillan, London, 1971, p. 433.
- 11 A. F. Psaila, Ph.D. Thesis, University of Exeter, 1977.
- 12 E. W. Abel, S. K. Bhargava and K. G. Orrell, *Prog. Inorg. Chem.*, 1984, **32**, 1.
- 13 T. G. Appleton, H. C. Clark and L. E. Manzer, *Coord. Chem. Rev.*, 1973, **10**, 335.
- 14 K. Kite and A. F. Psaila, *J. Organomet. Chem.*, 1992, **441**, 159.
- 15 P. J. Heard, Ph.D. Thesis, University of Exeter, 1994.
- 16 K. Kite and A. F. Psaila, University of Exeter, unpublished work.
- 17 G. W. Smith, *J. Chem. Phys.*, 1963, **39**, 2031.
- 18 G. W. Smith, *J. Chem. Phys.*, 1964, **42**, 435.

Received 25th April 1996; Paper 6/02896I